

## Geochemical Evolution of Great Salt Lake, Utah, USA

Blair F. Jones · David L. Naftz · Ronald J. Spencer · Charles G. Oviatt

Received: 13 June 2008 / Accepted: 10 November 2008 / Published online: 2 December 2008  
© U.S. Geological Survey 2008

**Abstract** The Great Salt Lake (GSL) of Utah, USA, is the largest saline lake in North America, and its brines are some of the most concentrated anywhere in the world. The lake occupies a closed basin system whose chemistry reflects solute inputs from the weathering of a diverse suite of rocks in its drainage basin. GSL is the remnant of a much larger lacustrine body, Lake Bonneville, and it has a long history of carbonate deposition. Inflow to the lake is from three major rivers that drain mountain ranges to the east and empty into the southern arm of the lake, from precipitation directly on the lake, and from minor groundwater inflow. Outflow is by evaporation. The greatest solute inputs are from calcium bicarbonate river waters mixed with sodium chloride-type springs and groundwaters. Prior to 1930 the lake concentration inversely tracked lake volume, which reflected climatic variation in the drainage, but since then salt precipitation and re-solution, primarily halite and mirabilite, have periodically modified lake-brine chemistry through density stratification and compositional differentiation. In addition, construction of a railway causeway has restricted circulation, nearly isolating the northern from the southern part of the lake, leading to halite precipitation in the north. These and other conditions have created brine differentiation, mixing, and fractional precipitation of salts as major factors in solute evolution. Pore fluids and diagenetic reactions have been identified as important sources and especially sinks for  $\text{CaCO}_3$ , Mg, and K in the lake, depending on the concentration gradient and clays.

---

B. F. Jones (✉)

Water Resources Discipline, US Geological Survey, 12201 Sunrise Valley Drive,  
Reston, VA 20192, USA  
e-mail: bfjones@usgs.gov

D. L. Naftz

Water Resources Discipline, US Geological Survey, 2329 Orton Circle, Salt Lake City,  
UT 84119, USA

R. J. Spencer

Geoscience, University of Calgary, 2500 University Drive Northwest, Calgary, AB, Canada T2N 1N4

C. G. Oviatt

Department of Geology, Kansas State University, Manhattan, KS 66506, USA

**Keywords** Lakes · Saline · Evaporation · Mixing · Calcium bicarbonate · Sodium chloride · Precipitation · Re-solution · Halite · Mirabilite · Calcite · Dolomite · Mg-silicate · Diffusion · Pore-fluids · Diagenesis · Climate

## 1 Introduction

The geochemical evolution of Great Salt Lake (GSL), as with other major inland salt water bodies, has involved a large interdisciplinary complex of factors of variable significance. The most important influences include meteoric precipitation, weathering, groundwater, evaporation, mineral precipitation-dissolution, and biotic activity. The dimensional properties of the lake are listed in Table 1, and play a major role in the geochemistry, hydrology, and associated climate of the lake. Input of major dissolved constituents is most simply and generally described by mixing dilute calcium bicarbonate stream waters with NaCl-dominated ground waters and hydrothermal springs (Spencer et al. 1985a, b)

In this paper we present a review of the hydrologic history of the lake basin in terms of lake level changes that occurred in response to changes in the balance between inflow and outflow. The hydrologic history is based on a review of previous work, primarily on ancient shorelines. We then present information on the chemistry of the various inflow components to the system. This is followed by a review of the concepts employed in interpreting the geochemical evolution of brines. The geochemical evolution of the lake water chemistry within the basin is discussed in the context of the changes in the hydrologic history and changes in relative inputs of inflow components with different chemical compositions in response to the hydrologic changes employing the principles of brine evolution. The discussion of the geochemical evolution of the lake above provides a context for the discussion of the modern lake that follows.

## 2 Hydrologic History of the Basin

The lake basin now occupied by GSL began forming in response to tectonic extension in the eastern Basin and Range Province in the middle Tertiary (Miller 1991). Lake sediments of Miocene age have been identified in the basin, both in deep cores from the basin center and in outcrops of faulted offshore sediments on the basin margins (Miller 1991). Most previous work on the lacustrine history of the basin has focused on the late Pleistocene (Gilbert 1890; Scott et al. 1983; Spencer et al. 1984; Oviatt et al. 1992), but older Pleistocene lakes have also been investigated (Kowalewska and Cohen 1998; Balch et al. 2005).

A summary of the late-Pleistocene history of Lake Bonneville is of particular interest here as the precursor to hypersaline GSL. Prior to about 28,000 <sup>14</sup>C year B.P. the lake level was apparently similar to Holocene GSL, although no shorelines of this age have been identified and dated. Pre-Bonneville sediments in cores from the floor of GSL are composed of laminated mud and fine sand, and both saline-tolerant ostracodes and brine-shrimp fecal pellets are present in different samples, but the sediments are not dominated by brine-shrimp fecal-pellet mud as are Holocene GSL sediments (Spencer et al. 1984; Oviatt and Thompson 2008, unpublished data).

Changes in the inflow/outflow balance to the basin resulted in the rise of Lake Bonneville to altitudes above those comparable to modern GSL after about 28,000 <sup>14</sup>C year

**Table 1** Dimensional properties of Great Salt Lake

Present elevation		Surface area		Volume	
<i>Size</i> <sup>a</sup> 4196 ft; 1279 m		1200 mi <sup>2</sup> ; 31,000 ha		1.5 × 10 <sup>7</sup> ac-ft; 1.9 × 10 <sup>10</sup> m <sup>3</sup>	
Evaporation (1931–1976)		River inflow (1931–1976)		Rainfall (1931–1976)	
2.9 × 10 <sup>6</sup> ac-ft; 3.6 × 10 <sup>10</sup> m <sup>3</sup>		1.9 × 10 <sup>6</sup> ac-ft; 2.3 × 10 <sup>9</sup> m <sup>3</sup>		0.9 × 10 <sup>6</sup> ac-ft; 1.1 × 10 <sup>9</sup> m <sup>3</sup>	
<i>Water budget</i> <sup>a</sup>		TDS high		TDS low	
2.9 × 10 <sup>6</sup> ac-ft; 3.6 × 10 <sup>10</sup> m <sup>3</sup>		1.9 × 10 <sup>6</sup> ac-ft; 2.3 × 10 <sup>9</sup> m <sup>3</sup>		0.9 × 10 <sup>6</sup> ac-ft; 1.1 × 10 <sup>9</sup> m <sup>3</sup>	
TDS average		TDS high		TDS low	
<i>Chemistry</i> <sup>a</sup>		~28% North arm; ~27% south arm		~28% North arm; ~6% south arm	
28% North arm; 12% south arm		~28% North arm; ~27% south arm		~28% North arm; ~6% south arm	

<sup>a</sup> Sources of data: Arnow and Stephens (1990) and <http://ut.water.usgs.gov/greatsaltlake/>

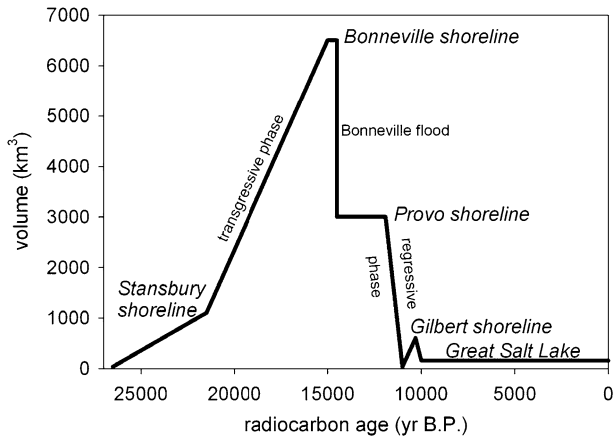


**Fig. 1** Changes in lake volume in the Bonneville basin versus radiocarbon age. Large swings in volume during the transgressive phase while Lake Bonneville occupied the closed basin are not shown. Major mappable shorelines are indicated. Note that the hypersaline Great Salt Lake fluctuated during the Holocene within a narrow volume range (about 38–317 km<sup>3</sup>). Data from Currey (1990 Figure 16), Oviatt (1997), and unpublished data

B.P. The lake continued to transgress to higher altitudes until it reached the low point on the basin rim and began to overflow, shortly after about 15,300 <sup>14</sup>C year B.P. (Oviatt et al. 1992; Oviatt 1997) (Fig. 1). During the transgressive phase of Lake Bonneville, lake level and lake volume progressively increased, and the water became more dilute. The lake occupied a hydrographically closed basin for its entire transgressive phase and fluctuated continuously in level, undergoing a series of major oscillations. The prominent Stansbury shoreline formed during one of these oscillations; these oscillations are not depicted in Fig. 1.

Lake Bonneville briefly overflowed into the Snake River drainage at its highest level and formed the Bonneville shoreline. Lake Bonneville catastrophically dropped about 100 m in altitude as the overflow threshold washed out in an event known as the Bonneville flood (Gilbert 1890; Oviatt et al. 1992; O'Connor 1993). The lake continued to discharge across a bedrock-floored threshold into the Snake River drainage for approximately 2500 years, during which time the Provo shoreline formed throughout the basin (Gilbert 1890; Godsey et al. 2005). The rapid closed-basin regressive phase began about 12,000 <sup>14</sup>C year B.P. and dropped the lake to altitudes comparable to modern GSL by about 11,000 <sup>14</sup>C year B.P. (Oviatt et al. 2005). A brief rise to the Gilbert shoreline at roughly 10,000 <sup>14</sup>C year B.P. was followed by Holocene fluctuations of GSL within an altitude range of 6 m (1280–1286 masl), and a volume range of about 40–300 km<sup>3</sup> (Fig. 1).

During the transgressive phase of Lake Bonneville, lake level and lake volume progressively increased, and the water became more dilute. In sediment cores from GSL that cover the transgressive phase, laminations containing large percentages of endogenic aragonite are interbedded with the dominantly calcite mud (Spencer et al. 1984; Oviatt and Thompson 2008 unpublished data). Aragonite laminations may indicate times when lake volume declined and the Mg to Ca ratio increased, possibly in response to an influx of water from the Sevier arm of the lake, where the river inflow has a relatively high Mg/Ca ratio (Oviatt et al. 1994; Pedone 2004).

Aragonite replaces calcite as the dominant mineral in post-Provo, regressive-phase sediments. This was caused by lake-volume decrease and progressive removal of Ca from the water as carbonate minerals precipitated, leading to an increase in the Mg/Ca ratio, and a shift from calcite to aragonite precipitation (Spencer et al. 1984). Aragonite dominates the carbonate mineral assemblage throughout the Holocene sedimentary column of GSL (Spencer et al. 1984; Oviatt and Thompson 2008 unpublished data). The end of the regressive phase of Lake Bonneville, prior to the development of the Gilbert shoreline (Fig. 1), marks the beginning of the GSL in something close to its modern configuration.

### 3 Geochemistry of Inflowing Waters

The lithology and distribution of rocks and sediments available for weathering, and groundwater residence times, exert fundamental controls on the initial chemistry of the inflow into closed lake basins. The chemical pathways taken by evolving saline water and the nature of evaporitic precipitates is largely set by initial dilute water chemistry. The chemical evolution can be associated with a few fundamental rock types, their mode of reaction with dilute waters, and the resulting relation in the proportion of major cations and anions, as shown in Fig. 2 (Jones and Deocampo 2003). The GSL basin offers a wide variety of reactive lithologies ranging from Precambrian and Paleozoic rocks in the Wasatch mountains in the east to Tertiary sediments and volcanic rocks in the basins in and west of the GSL Desert. Areal variation in precipitation, runoff, river discharge, and groundwater input influence the lake chemistry and solute evolution because of exposure to different lithologies.

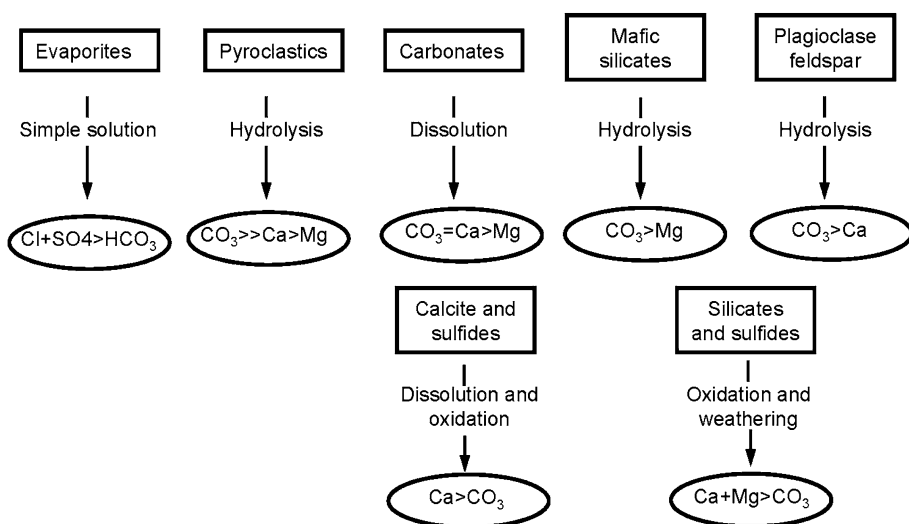


**Fig. 2** Schematic representation of general fluid compositions produced by weathering of different rock types, with relative solubility decreasing to the right. Solutes (Ca, Mg, SO<sub>4</sub>, CO<sub>3</sub>) refer to total aqueous species in equivalents, and CO<sub>3</sub> refers to all aqueous CO<sub>2</sub> species. Sulfide weathering is represented on a second level to demonstrate the possibility of competing weathering processes that can reverse the (Ca + MgCO<sub>3</sub>) ratio, an important early determinant of brine evolution pathways. Modified from Jones and Deocampo (2003)

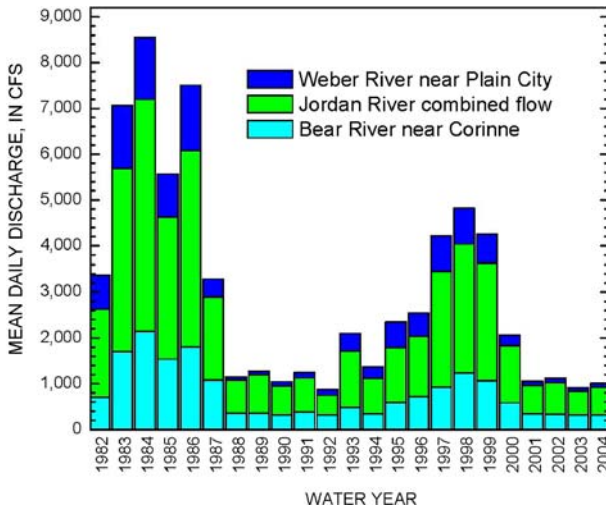


**Fig. 3** Mean daily discharge of the Bear, Jordan, and Weber Rivers from 1982 through 2004

The water and solutes of GSL depend primarily on the variable balance between evaporation and the three major rivers which provide more than 90 percent of the inflow to the lake (inflow percentages are: Bear + Weber = 79%; Jordan = 13%; see Fig. 3). All these waters are fundamentally of the calcium bicarbonate type, but vary somewhat characteristically in the secondary major constituents. To the north the Bear River typically contains a higher proportion of sodium carbonate obtained in its upper watershed, whereas the principle drainages to the south, which coalesce in Utah Lake and thence provide the Jordan River inflow to GSL, tend to carry more sulfate. The Weber River flowing directly out of the Wasatch Range to the east is generally the most dilute inflow, reflecting the predominance of silicate rocks in the drainage. An important solute source in the past was the Sevier River, which flowed into the southern part of Lake Bonneville at times of high lake level and provided marine salts, particularly magnesium sulfo-chloride, to the precursor of the GSL system (Feth 1960). Spencer et al. (1985a) have emphasized the importance of hydrothermal springs at low flow, as represented by NaCl-enriched inflow (to the Bear) from the Malad River, despite the relatively small discharge. Similar mixed NaCl-type hydrothermal springs and groundwaters were described by Cole (1982) on the east shore area of the lake. A summary of representative inflow compositions to GSL analyzed prior to the record rise in lake stage in the mid 1980s is given in Spencer et al. (1985a). Representative analyses of the major rivers taken since are given in Table 2. Data on chloride and H<sub>2</sub>O isotopes in wells and a few hot springs in the Weber delta—east shore (GSL) area were presented by Cole (1982).

#### 4 Geochemical Evolution of Brines—Concepts

Evaporative concentration is the dominant mechanism effecting mineral formation and solute evolution in closed basin systems (Jones 1966). Additional factors, including mixing and associated smaller scale processes (degassing, temperature change) also influence sequential mineral saturation and precipitation. The concept of “chemical divides” in the

**Table 2** Representative recent analyses of the three major inflows to Great Salt Lake, the Bear, Weber, and Jordan Rivers

Site	Date	Conductance (µs/cm)	HCO <sub>3</sub> <sup>-</sup> (mg/l)	Cl (mg/l)	SO <sub>4</sub> (mg/l)	Na (mg/l)	Mg (mg/l)	K (mg/l)	Br (mg/kg)	Ca (mg/kg)	Si (mg/kg)	B (mg/kg)	Sr (µg/l)	Li (µg/l)		
<i>Chemical analyses of major inflows</i>																
Weber River	04/18/00	515	208	50.7	19.8	32.6	14.6	3.75		45.4	7.72					
Bear River	04/26/00	790	259	107	30.9	72.1	24.1	7.13		50.8	10					
Jordan River	04/18/00	1350	276	185	189	139	43.1	11.9		68	18.5	254	953	106		
Site	Depth (m)	Date	Density (g/cm <sup>3</sup> )	Specific Gravity	HCO <sub>3</sub> <sup>-</sup> (mg/l)	Cl (%)	SO <sub>4</sub> (%)	Na (%)	Mg (%)	K (%)	Br (mg/kg)	Ca (mg/kg)	Si (mg/kg)	B (mg/kg)	Sr (mg/kg)	Li (mg/kg)
<i>Chemical analyses of Great Salt Lake (Gilbert Bay)</i>																
3510	1	11/14/02	1.0979	1.0998	467	7.18	0.80	4.11	0.40	0.23	54	189	<5	10	2.3	18
3510	6.5	11/14/02	1.1007	1.1027	462	7.43	0.83	4.38	0.42	0.24	60	189	<5	11	2.4	19
3510	8	11/14/02	1.1281	1.1301	392	9.75	1.08	5.25	0.52	0.29	61	190	<5	15	2.3	23
Normative salt assemblage																
Normative salts-percent																
Mole																
Weight (anhy)																
Simple salts-percent																
Mole																
Weight																
<i>SNORM calculation results for Great Salt Lake (site N1022 at 1 m depth)</i>																
Halite		NaCl		91.04208		75.29392		81.71210		Na <sub>2</sub> Cl <sub>2</sub>		81.41959				81.85606
Carnallite		KMgCl <sub>3</sub> · 6H <sub>2</sub> O		3.02660		11.89920		7.89064		K <sub>2</sub> Cl <sub>2</sub>		2.70671				3.47108
Kieserite		MgSO <sub>4</sub> · H <sub>2</sub> O		4.01470		7.85958		7.41910		MgCl <sub>2</sub>		7.91425				6.48159
Bischofite		MgCl <sub>2</sub> · 6H <sub>2</sub> O		1.39819		4.02208		2.04452		CaSO <sub>4</sub>		0.43649				0.51098
Anhydrite		CaSO <sub>4</sub>		0.24404		0.47002		0.51009		MgSO <sub>4</sub>		7.18075				7.43217
Magnesite		MgCO <sub>3</sub>		0.19133		0.22823		0.24768		MgCO <sub>3</sub>		0.34222				0.24812

Table 2 continued

Normative salt assemblage	Normative salts-percent		Simple salts-percent	
	Mole	Weight	Mole	Weight
–				
Indirite	0.06930	0.12546	0.11698	
Celestite	0.01236	0.09786	0.05493	
	0.00140	0.00365	0.00396	
Total	100.0	99.9	100.0	100.0
<i>SNORM calculation results for seawater</i>				
Halite	88.06538	70.08583	78.09516	Na <sub>2</sub> Cl <sub>2</sub>
Bischofite	4.46484	12.35450	6.45203	K <sub>2</sub> Cl <sub>2</sub>
Carnallite	1.91924	7.25857	4.94396	MgCl <sub>2</sub>
Kieserite	3.35215	6.30920	6.11496	CaSO <sub>4</sub>
Anhydrite	1.93415	3.58141	3.99069	MgSO <sub>4</sub>
Magnesite	0.22371	0.25654	0.28586	MgCO <sub>3</sub>
Indirite	0.01289	0.09815	0.05657	
Celestite	0.01747	0.04364	0.04863	
Sellaite	0.00682	0.00578	0.00644	
–	0.00245	0.00427	0.00408	
Nitromagnesite	0.00044	0.00153	0.00099	
Wagnerite	0.00012	0.00026	0.00029	
Salammoniac	0.00031	0.00023	0.00025	
Barite	0.00003	0.00009	0.00010	
Total	100.0	100.0	100.0	100.0

Recent analyses of the central south arm of Great Salt Lake (Gilbert Bay) are also given, illustrating compositional differences at the top and bottom of the lower stratified layer. Also included is a SNORM calculation comparison of analyses for the Great Salt Lake and seawater

evolution of closed basin waters was first described by Hardie and Eugster (1970). This concept is based on the idea that mineral precipitation from waters increasing in salinity as a result of evaporative concentration is controlled by the solubility of minerals. Most surface waters have a relatively simple major element composition. There are four major cations, Na, Ca, K, and Mg; and four major anions,  $\text{HCO}_3$ ,  $\text{CO}_3$ ,  $\text{SO}_4$ , and Cl. There are a limited number of salts that can be made from these building blocks. Chloride is the most conservative element in solution and the behavior of the other major ions on evaporative concentration can generally, but not specifically, be assessed by reference to Cl content (Eugster and Jones 1979). The least soluble minerals that can be obtained from the composition of most surface waters are the alkaline-earth carbonates, followed by the calcium sulfates. The precipitation of a mineral is controlled by the solubility of that mineral, the cation and anion involved both contribute to the precipitate and are lost from the solution in equal proportion. The solubility product of the cation and anion must be constant, so as the mineral precipitates, unequal amounts remain in solution and the constituent of greater proportion becomes dominant in solution on further concentration, i.e., during calcite precipitation an increase in Ca is accompanied by a decrease in  $\text{CO}_3$  or vice versa. Thus, early precipitation of calcium carbonate determines whether the remaining solution will become carbonate rich or poor. The concept of brine evolution during evaporative concentration can be illustrated with a flow chart such as the one illustrated on Fig. 4, which is modified from Eugster and Hardie (1978), adapted to GSL, and based on relative mineral solubility.

The early precipitation of alkaline-earth carbonates is a crucial step in understanding brine evolution. There are several alkaline-earth carbonates present in many closed basin sediments. Among these are calcite, Mg-bearing calcite (less than about 12 mole percent Mg), and aragonite. All of these phases have relatively low solubility. Carbonates with higher magnesium contents such as dolomite and magnesite also have low solubility, but are not common as primary precipitates in closed basin sediments, and are rare or absent as primary precipitates during the early stages of evaporative concentration. Calcium is preferentially removed from solution relative to magnesium during the precipitation of calcite, Mg-bearing calcite and aragonite, resulting in an increase in the ratio of Mg to Ca in solution during precipitation of these minerals. Experimental work by Fuchtbauer and Hardie (1976) shows a precipitation sequence from calcite to Mg-bearing calcite to aragonite with increasing Mg to Ca in solution. This is expected to occur in closed basin systems as inflow waters with relatively low Mg to Ca in solution are concentrated and alkaline earth carbonates precipitate.

Perhaps the easiest technique for applying the “chemical divide” concept in the prediction of solute evolution pathways is by use of the “Spencer Triangle” (Fig. 5). The system  $\text{Ca-SO}_4\text{-(CO}_3 + \text{HCO}_3)$  can be illustrated in a ternary phase diagram. The diagram is constructed by placing Ca,  $\text{SO}_4$ , and  $(\text{CO}_3 + \text{HCO}_3)$  in equivalents at the corners of a triangular diagram. The diagram uses equivalents as units of charge concentration inasmuch as the maintenance of charge balance is a crucial, but often overlooked, control during mineral precipitation. Therefore, the composition of calcite (as well as aragonite) lays half way between the Ca and  $(\text{CO}_3 + \text{HCO}_3)$  corners; there are equal equivalents of Ca and  $(\text{CO}_3 + \text{HCO}_3)$  in calcite. The composition of gypsum (as well as anhydrite) lays half way between the Ca and  $\text{SO}_4$  corners; there are equal equivalents of Ca and  $\text{SO}_4$  in gypsum. The body of this phase diagram is the primary precipitation field for calcite (Mg-bearing calcite and aragonite may also precipitate in this field). Waters can be plotted on this diagram using the equivalent concentrations of Ca,  $\text{HCO}_3$  plus  $\text{CO}_3$  and  $\text{SO}_4$  in the waters. The evolution of these waters may then be followed.

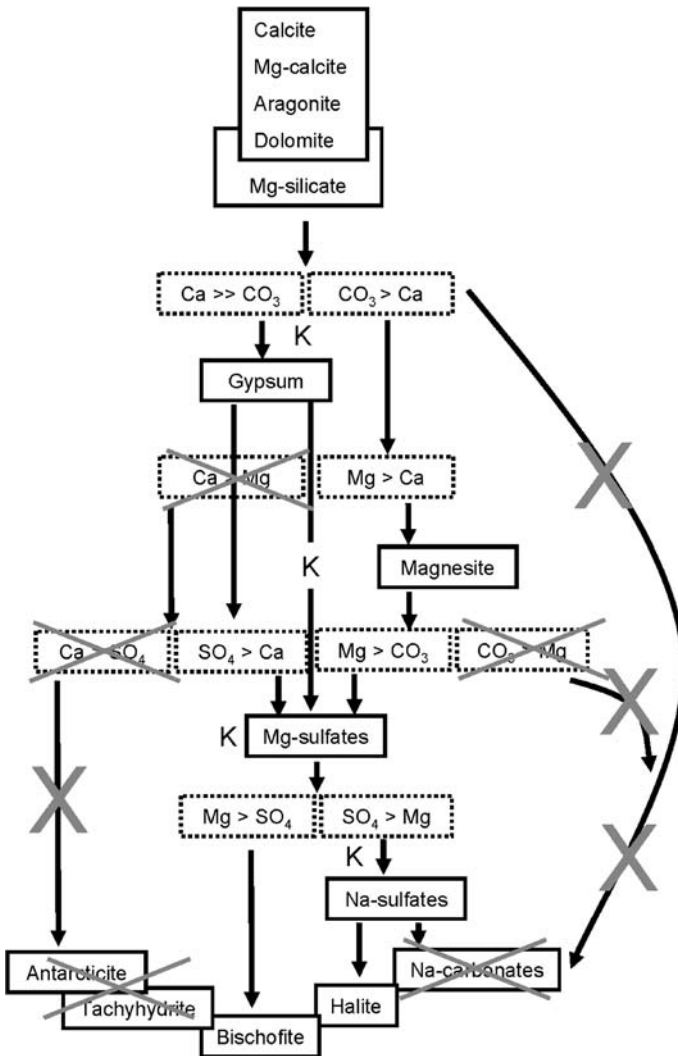


**Fig. 4** Flowchart of idealized evolution of a closed basin brine with increasing evaporative concentration downward modified to illustrate specific conditions for the Great Salt Lake. Solute constituents are indicated by dashed boxes, and mineral precipitates are indicated by solid boxes (after Eugster and Hardie 1978; Jones and Deocampo 2003)

The first mineral to precipitate from a concentrating water is determined by its position with respect to the primary precipitation field for minerals on the ternary phase diagram in Fig. 5. The body of this phase diagram is the primary precipitation field for calcite. Therefore, the first mineral to precipitate from waters that plot within the body of the triangle is calcite (or possibly Mg-bearing calcite or aragonite). During mineral precipitation the composition of the water moves directly away from the composition of the mineral. For instance, waters at points 1 and 2 on Fig. 5 will precipitate calcite and move directly away from the calcite compositional point. Continued evaporative concentration and calcite precipitation results in migration of the water composition to the join between

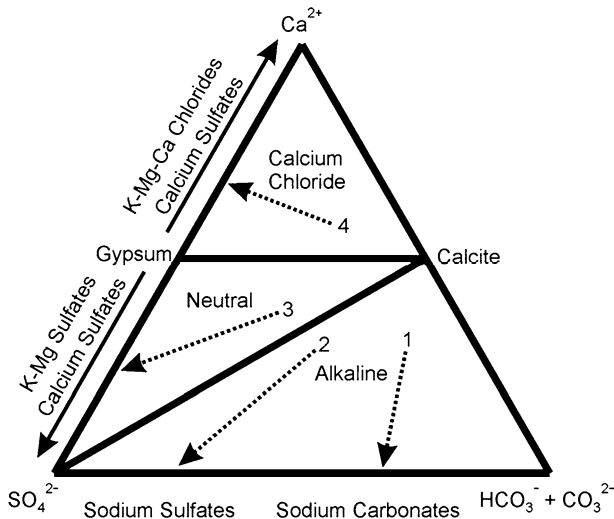


**Fig. 5** The “Spencer Triangle,” ternary phase diagram in the system Ca–SO<sub>4</sub>–HCO<sub>3</sub>, with compositional trends on evaporation indicated. For further explanation, see text

HCO<sub>3</sub> plus CO<sub>3</sub> and SO<sub>4</sub> as indicated by the arrows in Fig. 5. These waters become depleted in Ca during the precipitation of calcite; a portion of the HCO<sub>3</sub> and CO<sub>3</sub> and SO<sub>4</sub> remain in solution after calcite precipitation. These waters eventually may precipitate a number of more soluble salts, including sodium carbonate and/or sodium sulfate salts, but not calcium sulfate (gypsum). Waters near composition 1 precipitate sodium carbonates prior to sodium sulfate and waters near composition 2 precipitate sodium sulfate prior to sodium carbonate. All waters may precipitate halite (and other salts) at some point (see Spencer and Hardie 1990, for more details).

There are three distinct compositional fields separated by two chemical divides as a result of the precipitation of relatively insoluble minerals in the system displayed in Fig. 5. The join between the calcite compositional point and the SO<sub>4</sub> apex represents the divide between “Alkaline” and “Neutral” waters, and the join from calcite to gypsum represents the divide between “Neutral” and “Calcium Chloride” waters. Neutral waters, such as at composition 3 on Fig. 5, precipitate calcite and move directly away from the calcite composition. Continued evaporative concentration and calcite precipitation brings these waters to the gypsum stability field located along the join between Ca and SO<sub>4</sub> in Fig. 5. Waters are depleted in HCO<sub>3</sub> and CO<sub>3</sub> along this join and gypsum is the dominant precipitate. Waters move along the phase boundary away from the gypsum compositional point, toward the SO<sub>4</sub> corner of the diagram. Waters are depleted in Ca and further concentration leads to the precipitation of halite and a variety of other salts including K and Mg sulfates and chlorides.

Calcium chloride waters such as at composition 4 on Fig. 5, precipitate calcite and move directly away from the calcite composition. Continued evaporative concentration and calcite precipitation brings these waters to the gypsum stability field located along the join between Ca and SO<sub>4</sub> in Fig. 5. Waters are depleted in HCO<sub>3</sub> and CO<sub>3</sub> along this join and gypsum is the dominant precipitate. Waters move along the phase boundary away from the gypsum compositional point, toward the Ca corner of the diagram. Waters are depleted in

SO<sub>4</sub> and further concentration leads to the precipitation of halite as well as K, Mg, and Ca chlorides.

## 5 Geochemical Evolution of GSL

Spencer et al. (1985b) developed a geochemical model of the solute evolution in the basin over the last 35,000 years using existing data for lake stage, surface area, volume, evaporation, and inflow. The major solute sources under the hydrologic conditions considered were atmospheric precipitation, river waters, and hydrothermal springs. The estimates of the total input over 35,000 years are given in Table 3.

Sediment from mid-lake cores that cover the transgressive phase (Fig. 1) varies from laminated to mottled to massive in appearance. The mineralogy of the sediment is dominated by detrital quartz (~50%) and detrital clay minerals (~30%) and lesser amounts of endogenic low Mg calcite (<20%) (Spencer et al. 1984). The sediments contain fresh to brackish water ostracodes and well-preserved algal filaments. Overall the sediment is consistent with a rising lake receiving dilute, high discharge waters with a composition dominated by sodium bicarbonate-type waters as a result of the weathering of silicates (i.e., Bear and Weber Rivers), carrying significant detrital sediments load. The lake does not appear to have increased systematically in concentration during the transgressive stage, but rather to have become more dilute. However, there are short intervals of light colored sediment that contain small amounts of aragonite (10–15%) along with calcite (5–15%) and variable amounts of quartz (~10–50%) that punctuate this interval (Spencer et al. 1984). The aragonitic intervals are bracketed by ages of 21,050 <sup>14</sup>C year B.P. and 19,540 <sup>14</sup>C year B.P. (Thompson et al. 1990) and may represent fluctuations near the Stansbury shoreline (see Fig. 1). Oviatt and Thompson (2008 unpublished data) also report sediment within the transgressive interval containing large percentages of endogenic aragonite interbedded with the dominantly calcite mud. Aragonite laminations may indicate times when lake volume declined and the Mg to Ca ratio increased, although there is no indication of a progressive shift in the lake chemistry as seen in the major drawdown discussed below. These aragonitic intervals may be in response to an influx of water from the Sevier arm of the lake, where the river inflow has a relatively high Mg/Ca ratio (Oviatt et al. 1994; Pedone 2004).

**Table 3** Salt budget over 35,000 years (as calculated by Spencer et al. 1985b)

Sinks	Cl <sup>-</sup>	SO <sub>4</sub> <sup>2-</sup>	HCO <sub>3</sub> <sup>-</sup>	Na <sup>+</sup>	K <sup>+</sup>	Ca <sup>2+</sup>	Mg <sup>2+</sup>	SiO <sub>2</sub>
Lake brines	2.65	0.25	0.005	1.53	0.07	0.005	0.13	
Pore fluids	2.70	0.15	0.005	1.50	0.08	0.005	0.10	
Salts	0.21	0.80		0.53				
Sediment		0.40	22	0.13	0.04	7.4	0.64	0.96
Overflow loss	1.12	0.45	0.24	0.74	0.08	0.10	0.19	
Total sinks	6.68	2.05	22.25	4.43	0.27	7.51	1.06	0.96
Total input	6.90	2.36	12.26	4.54	0.36	3.52	0.87	0.50
Percentage of input accounted for	97	87	181	98	75	213	122	192

Sources and sinks for major dissolved species in Great Salt Lake inflow and brines. Salts include mirabilite and halite; sediment includes sulfides, carbonates, gypsum, and clays. Mass estimates given here are presented in 10<sup>15</sup> g

During the development of the Bonneville shoreline, the Bonneville flood, and the Provo shoreline (Fig. 1) the lake was overflowing into the Snake River drainage system. Therefore, from the perspective of the deep lake sediment and geochemical evolution of waters, this interval is grouped with the transgressive phase and was characterized by a relatively fresh lake receiving high discharge waters.

The regressive phase of the lake is clearly recorded in the mid-lake cores. The most dramatic changes in the mid-lake cores occur over a 25-cm interval of sediment. At the base of this interval the sediment mineralogy consists of detrital quartz (~55%), detrital clay minerals (~30%) and low Mg calcite (~15%), typical of the transgressive sediments described above. These sediments also contain ostracodes indicative of the freshest water conditions in the entire core record. Over an 8 cm interval the quartz content of the sediment drops systematically from 55% to 20%, while calcite content increases continuously from 15% to 55% and the Mg content of the calcite increases steadily from near zero to 11 mole percent. Immediately above this is a 2 cm interval containing about 50% aragonite, 5% calcite, 15% quartz, and 30% clay minerals. Above this is an interval of what appears to be reworked sediment with mud coated and abraded ostracodes. Brine shrimp cysts first appear in muds just below the coated ostracodes and initially even with some uncoated ones, but they are much more abundant above the carbonate coated ostracodes. This indicates that the lake had become saline and was reaching relatively low levels. The interval covering the regressive phase described above is bracketed by ages of 12,400  $^{14}\text{C}$  year B.P. and 11,970  $^{14}\text{C}$  year B.P. (Thompson et al. 1990).<sup>1</sup>

The regressive interval described above covers the precipitation of alkaline-earth carbonates during the rapid drawdown of the lake as a result of evaporative concentration. The sequence from calcite, through Mg-bearing calcite with increasing Mg-content to aragonite is consistent with the experimental work by Fuchtbauer and Hardie (1976) in response to an increase in the Mg to Ca ratio in solution as calcium is preferentially removed from waters to form the carbonates. The beginning of the evaporative phase chemistry is signaled by the increase in the amount of calcite and the Mg-content of the calcite. The shift from Mg-calcite to aragonite is simply a point in the continuous sequence. The lake continued to become more concentrated beyond this point as indicated by the presence of brine shrimp.

Lake levels appear to have also dropped above this stratigraphic level, to a point where the lake was divided by the bathymetric high shown south of Promontory Point on the bathymetric map in Fig. 6 into a north basin and a south basin. The major river inflow to the lake (Bear, Weber and Jordan) is south of this divide. Cores to the south of the divide contain up to 50 cm of finely laminated, organic-rich sediment. Cores along and near the divide contain about 15 cm of cemented aragonitic crusts. Bedded mirabilite ( $\text{Na}_2\text{SO}_4 \cdot 10\text{H}_2\text{O}$ ) is present north of the divide. The base of this interval is dated at 9680  $^{14}\text{C}$  year B.P. (Thompson et al. 1990) and appears to occur subsequent to the development of the Gilbert shoreline (Fig. 1).

The evolution of the lake waters during the regressive phase can be followed on the ternary phase diagram in Fig. 7a. The solutes in the lake prior to regression were dominated by input from waters entering the lake during the transgressive and overflow phases. These high discharge, meteoric waters were a mixture of Weber, Bear, Jordan and possibly Sevier river waters with a composition within the “Alkaline” field in the shaded triangle on

<sup>1</sup> In some cores the aragonite peak is replaced by a “dolomite” peak (primary XRD peak near 31 degrees 2-theta), and although aragonite does increase in this interval, “dolomite” is the dominant carbonate mineral. Could the “dolomite” be a secondary replacement of aragonite?

Fig. 7a. The waters migrated along the dashed line in Fig. 7b as a result of the precipitation of calcite, Mg-bearing calcite with increasing Mg-content, and aragonite during the regressive phase. The waters eventually reached the join between  $\text{HCO}_3$  plus  $\text{CO}_3$  and  $\text{SO}_4$  and precipitated mirabilite, but not gypsum. Spencer et al. (1985b) suggest that mirabilite precipitation in the north basin initiated during winter “chill out” (which has been observed temporarily in recent times) and the beds possibly protected from dissolution by overlying stratification resulting from mineral precipitation and sedimentation.

The chemistry of the lake has changed through time. Modern GSL brines are within the “Neutral” field as indicated on Fig. 7b. Lake levels appear to have fluctuated near present day levels during the past 9000 years. Sediments are dominated by brine shrimp pellets

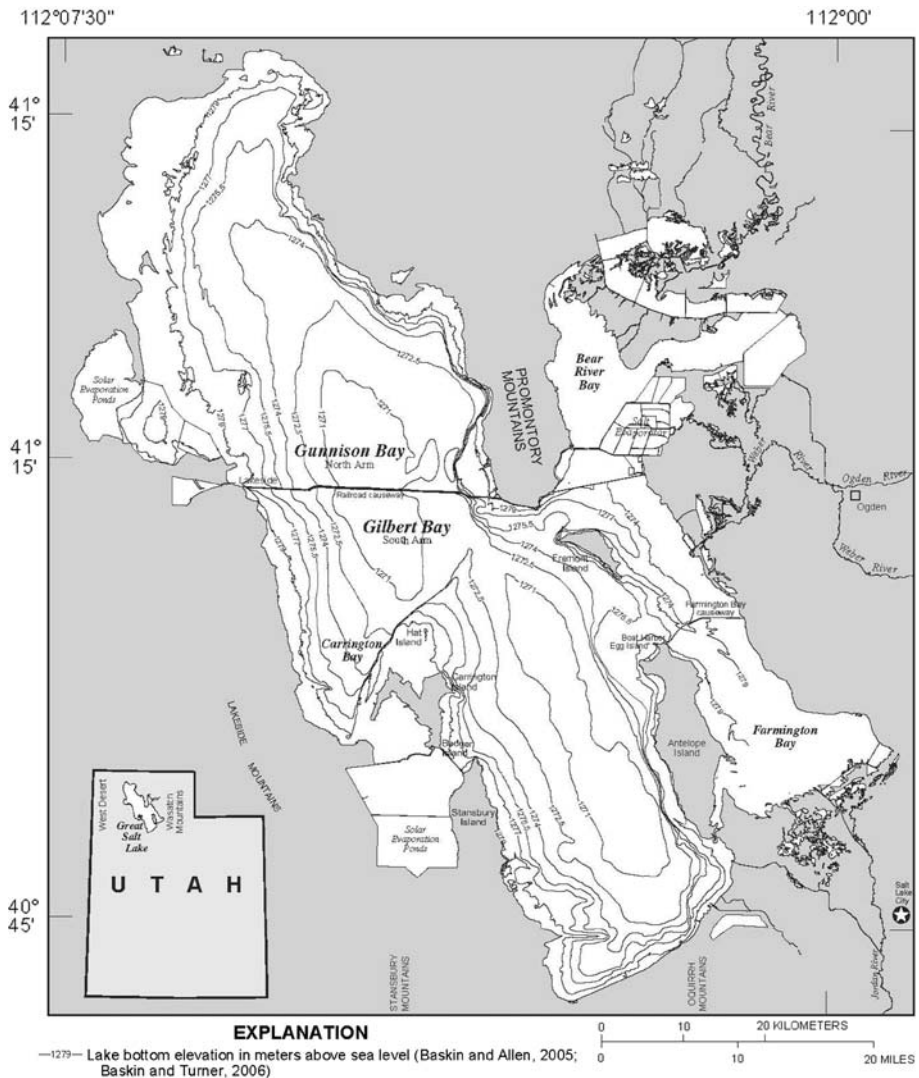


**Fig. 6** Location and bathymetry of Great Salt Lake, Utah. From Baskin and Allen (2005)

composed of aragonitic mud. Disrupted, chemoturbated sediments indicate the growth and dissolution of mirabilite throughout the interval. However, gypsum is present as discoidal crystals, likely of diagenetic origin, within the upper 1.5 m of sediment, above the Mazama tephra with an age of 6730 <sup>14</sup>C year B.P. (7627 cal year B.P.) (Zdanowicz et al. 1999), and as a primary precipitate in the upper 10 cm of sediment. The presence of gypsum indicates a “Neutral” composition of the brines. Thus, there is a difference in mineral precipitation sequence which can be explained in terms of the composition of low versus high inflow discharge. The major inputs to the lake under low discharge conditions are the “Alkaline” waters of the Bear, Weber, and Jordan rivers, plus a contribution from springs, such as the Malad Springs, along the Wasatch front. The spring waters are of the “Calcium Chloride” type, see Fig. 7b. There is a much higher relative contribution of the “Calcium Chloride” solutes during low-discharge than at high-discharge conditions. The continued input of the spring water component during the 10,000–11,000 year low stand has resulted in the migration of the lake water chemistry into the neutral field, to a point where it follows the evaporation path indicated by the dotted line in Fig. 7b.

Continued input of Cl and Na from hydrothermal sources, evaporation, and re-cycling from peripheral mud flats results in increased concentration of these components in the lake, despite downward diffusion gradients (Fig. 8). In contrast, the diffusive fluxes of SO<sub>4</sub>, K, and Mg into the sediment are supplemented or enhanced by diagenetic reactions in the sediment. Sulfate reduction and some gypsum formation takes place variously in the sediment, whereas K fixation and Mg-silicate formation occurs in the clay fraction (Jones and Spencer 1999). Thus, input of SO<sub>4</sub>, K, and Mg is insufficient to keep up with removal. Mirabilite still occurs intermittently through brine chilling. According to Spencer et al. (1985b) the sequence expected from modern brines at 25°C is aragonite, small amounts of gypsum and glauberite, and then a large mass of halite. The variations in mineral precipitate sequences, the fossil mirabilite found in the sediment, and the halite dominance in salts precipitated at present are a testimony to the changing influence of input sources and sinks through time (Spencer et al. 1985b).

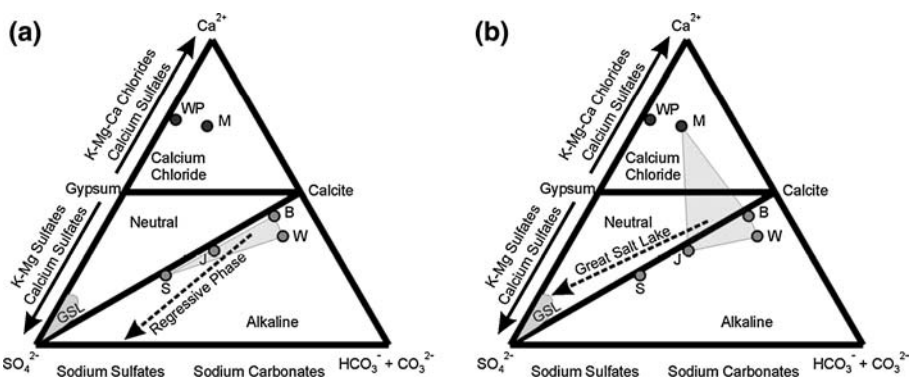
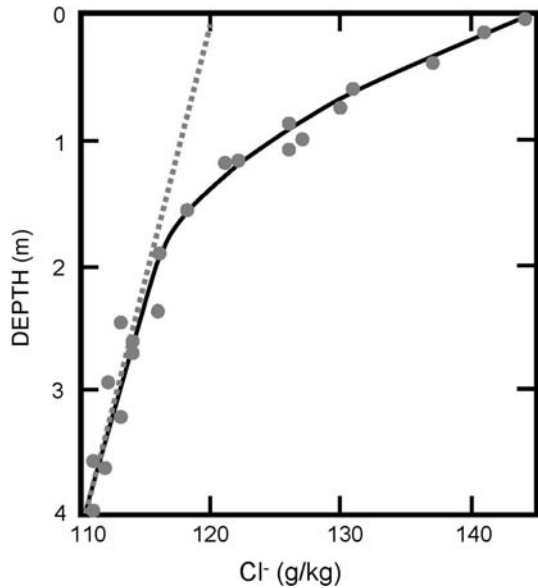


**Fig. 7** Two versions of the “Spencer Triangle” indicating pathways taken by specific compositions in the evolution of water precipitating calcite, with or without subsequent minor precipitation of gypsum (from Jones and Bodine 1987; Spencer and Hardie 1990). The dashed lines represent the compositional trends for the regressive phase of Lake Bonneville or for the modern Great Salt Lake. Individual points represent (B) Bear River, (W) Weber River, (J) Jordan River, (S) Sevier River, (M) Malad River, and (WP) West Pond overflow from Great Salt Lake into the Bonneville Desert. The shaded areas on the diagram represent the compositional range of mixtures of the major inflows

**Fig. 8** The chloride pore fluid analyses from the deepest portion of the northern south arm, GSL, as a function of depth. The dashed line is an estimated 1933 profile, prior to halite precipitation. The solid curve is the calculated diffusion profile, assuming the bottom waters remain near or at halite saturation from 1933 to 1980 (from Spencer et al. 1985a)



## 6 The Modern Lake System

In view of the strong influence of modeling on the sequences offered here, it is of interest to compare the results of computer calculations of evaporative concentration and salt precipitation using the model TEQUIL (Møller et al. 1997) by Kohler and White (2004) with the field determinations of Jones et al. (1997) in a sequence of commercial evaporation ponds (Fig. 9). For evaporative evolution of brine beginning with analyses of halite-saturated fluids from the north arm of GSL, the post-halite precipitation sequence of phases determined by computer or field collection was nearly identical. The computer sequence was anhydrite—glauberite—polyhalite—leonite—kainite—(kieserite—carnallite). X-ray diffraction analyses of field samples picked up traces of glauberite, but failed to detect polyhalite and leonite, though the latter was probably taken up in the formation of kainite, which was clearly the most abundant bitter salt. The identification of kieserite and carnallite at the end of the pond sequence sampled was questionable, but could not be separated from decreasing amounts of kainite. The  $\text{MgCl}_2$  brine of the last pond (#4) was too deliquescent to permit collection of precipitate.

Detailed information on historic changes in GSL elevation through time has been given by Arnow and Stephens (1990) (Fig. 10). Prior to about 1955 the lake concentration was inversely proportional to lake stage (volume). Significant precipitation of halite beginning around 1955 took control of the chloride concentration in the lake brines and resulted in a significant deviation of lake waters from the simple volume-concentration relationship (Fig. 10). Historic lake elevation changes have precipitated and re-dissolved salts, mostly halite, but also mirabilite ( $\text{Na}_2\text{SO}_4 \cdot 10\text{H}_2\text{O}$ ), leading to the formation of stratified brines. This has been the result of both evaporative concentration during drought periods and the construction of the railroad causeway across the lake in 1959. In addition to the causeway dividing the lake into a north and south arm, the south arm is further divided by a natural ridge into a north and south basin. As discussed in considerable detail by Spencer et al. (1985a), mineral precipitation, re-solution, fractionation, and mixing of brines have

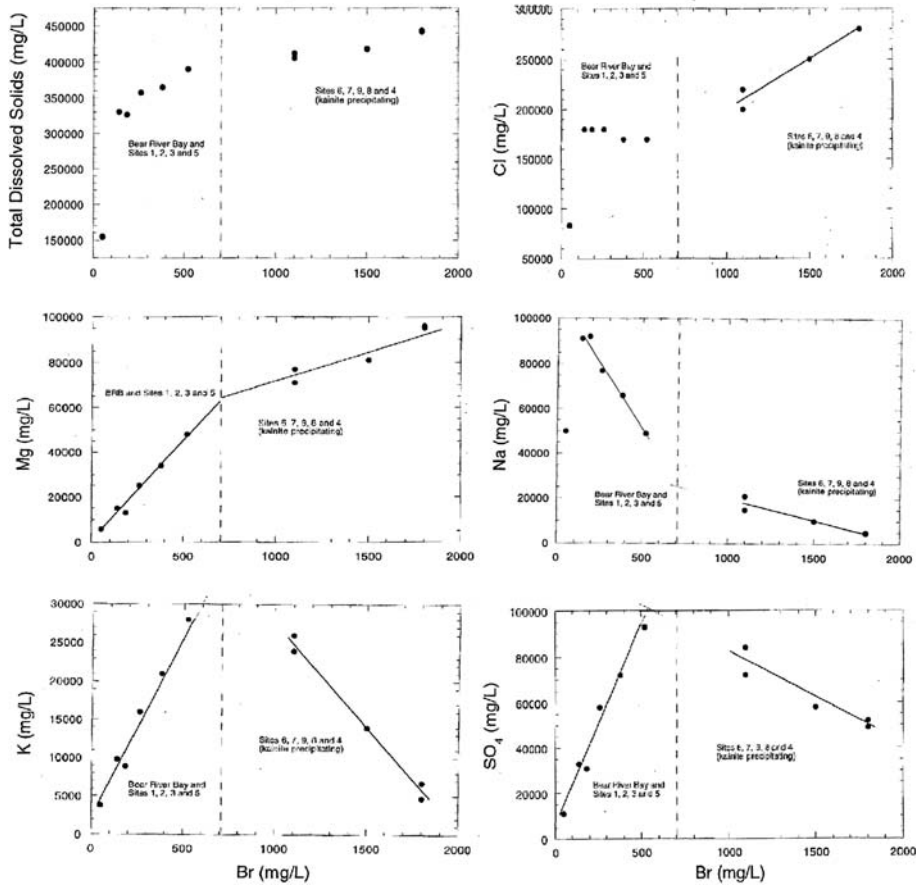


**Fig. 9** X-Y plots of major solutes vs. bromide for a sequence of evaporation ponds fed by fluids from the halite-saturated North Arm brine of Great Salt Lake, August 1996. Br is considered to be relatively conservative in solution, as indicated by the relation to TDS up to about 700 mg/kg (samples 1, 2, 3, 5). In contrast, the Br remains essentially constant vs. TDS in the more concentrated samples (6, 7, 8, 9, & 4—the most concentrated pond), although illustrating a positive relation with Cl & Mg, and a negative slope with Na, K, & Ca. However, all the major solutes show a pronounced change in slope of their relation with Br at the 700 mg/kg level, based on x-ray determinations on the more concentrated group, this concentration appears to mark the initial precipitation of kainite in this setting

profoundly affected brine composition and evolution. Using the data of Hahl and Mitchell (1963) Hahl and Handy (1969) and others, Spencer et al. (1985a) utilized chloride reference to analyze the historic changes in lake brine composition, development, and distribution. From this, it is clear that the mixing of fractionated brine bodies has become an important component of brine evolution.

Salt (NaCl) precipitation occurred during the drought of the 1930s (1935–1945) and again in the 1960s. In the South Arm the salt was apparently re-dissolved by 1972, but stayed saturated in the north arm until the large lake-level rise in the 1980s. From 1965 until 2002, there was a slight decline in SO<sub>4</sub>, Mg, K, and Ca, whereas Na and Cl increased. For the period 1966–1981 there was an increase in the relation of total dissolved solids (TDS) versus stage in the south arm and constancy in the north arm, until the heavy rains

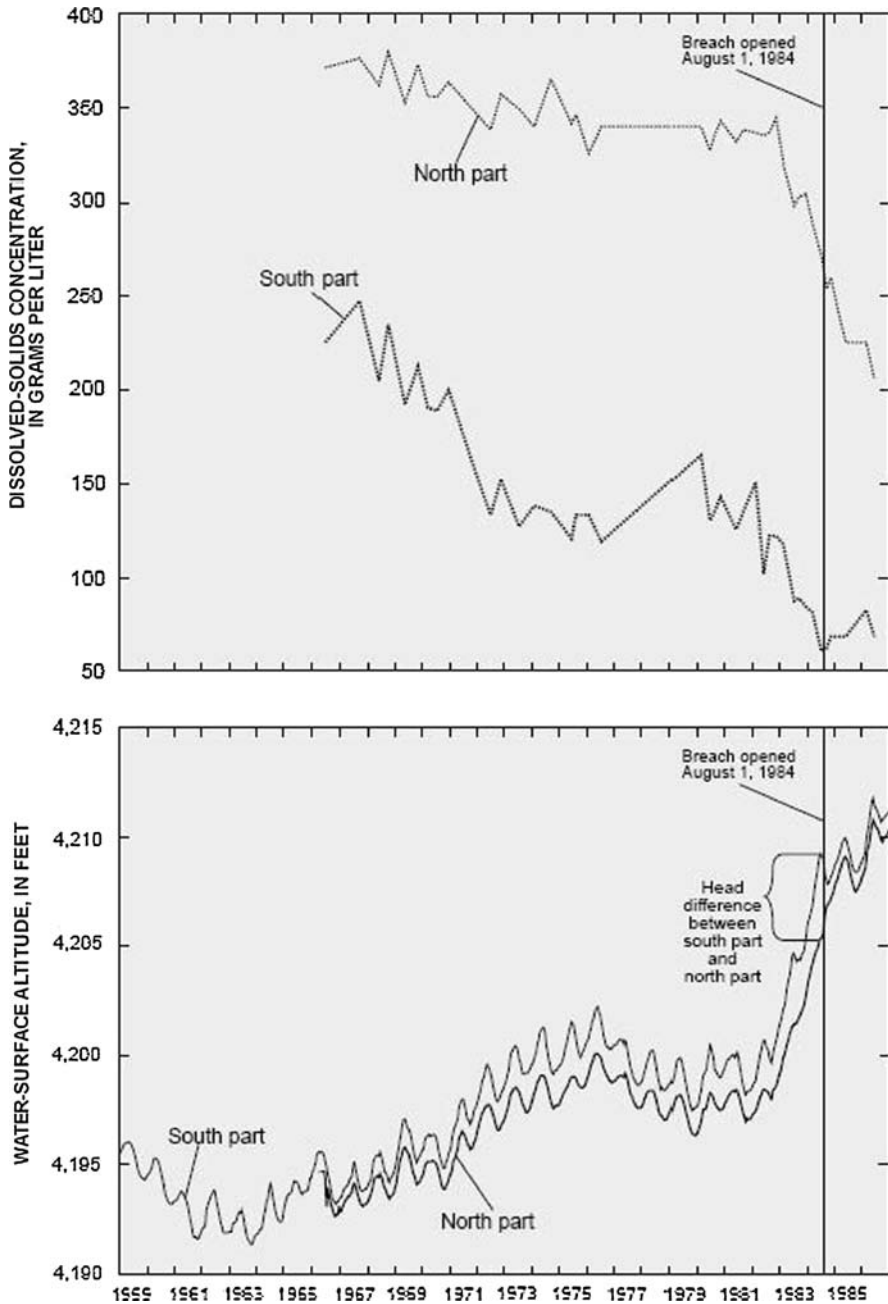


**Fig. 10** Changes in water level and salinity of the Great Salt Lake, 1847 to 1986. From Arnow and Stephens (1990 Fig. 3)

and South Arm inflow increased dramatically. Salt precipitation began again in the summer of 1992 and continued to the present (Gwynn 2002). Prominent minor elements (Br, B, Li) increased relative to NaCl. Exchange across the railroad causeway has kept the concentration trends similar. Bidirectional flow related to a brine interface existed across the causeway from pre-1966 until mid 1991 because of the lack of return flow thru the causeway and vertical mixing. Since 1992 the north arm has been at halite saturation, so there was no inverse relation to lake level. Since 1993 there has been only south to north flow or none at all. The lake-level rise since 1995 has increased the south to north surface flow, but compaction of fine-grained sediments in the causeway fill has shut off the underflow return. Movement southward of south arm bottom brine over the mid-lake ridge from the north to the south was noted by Hahl and Handy (1969).

Farmington Bay has apparently often been isolated from main GSL, but under average conditions, has a salinity about half of the main lake. The proportion of major ions is about the same as in the lake. The bay acts as a biological treatment lagoon for nutrients, N and P, from the Jordan River and sewage-treatment plants. Six mineral-extraction industries operate on the lake. These produce potash fertilizer, Mg metal, and Cl gas, as well as a variety of salts.

## 7 Geochemical Dynamics

As in all natural waters, the composition of any saline lake is dominated by less than ten major solutes, Na, K, Ca, Mg, Cl, SO<sub>4</sub>, dissolved inorganic carbon as HCO<sub>3</sub> + CO<sub>3</sub> and sometimes SiO<sub>2</sub>. Of these, Na is the most common cation, and often is nearly the only cation in solution. The short-term processes noted above mainly affect Na, SO<sub>4</sub>, and Cl, whereas Mg and K remain mostly solute conservative (lost only to long-term pore-fluid diffusion, diagenetic mineral formation in sediment, aerosols, or the mineral extraction industries). In the Great Basin, overall compositional trends can be described almost entirely in terms of the anions in saline waters (Jones 1966). However, Bodine and Jones (1986) found it more useful to classify saline waters according to normative analyses of their principal anion-cation associations based on relative mineral solubility. Further, in the latter stages of chemical evolution the ratios with respect to the alkalis and sulfo-chloride become more important, and it is advantageous to consider associations within the entire solute matrix. For this purpose, the computer program SNORM calculates the equilibrium salt assemblage expected for any water taken to dryness at 25°C and atmospheric *p*CO<sub>2</sub>. Thus, regardless of the initial composition, saline waters can be compared in terms of the total salt assemblage to be expected on complete evaporation, including the presence or absence of characteristic double salts. Using recalculation of the assemblage to “simple salts,” multiphase mineral assemblages can be reduced to simple characteristic cation-anion associations.

An example from the central northern section of the south arm of GSL in 2002 is given in comparison with seawater (Table 2). Though the salt assemblage is quite similar, differences in the normative proportions are readily recognized. Such analyses permit the evaluation of the effects of processes other than evaporative concentration on the chemical evolution of saline water by recognizing deviation from the projected assemblage. For instance, one can look for small variations in the residual, solute-conservative “simple salts” (specifically the K and Mg chlorides) calculated from the analyses representing a small portion or the entire area of GSL as sensitive indicators of solute modification processes. Results derived from lake analyses in 2002 are presented in Fig. 11a, b in terms

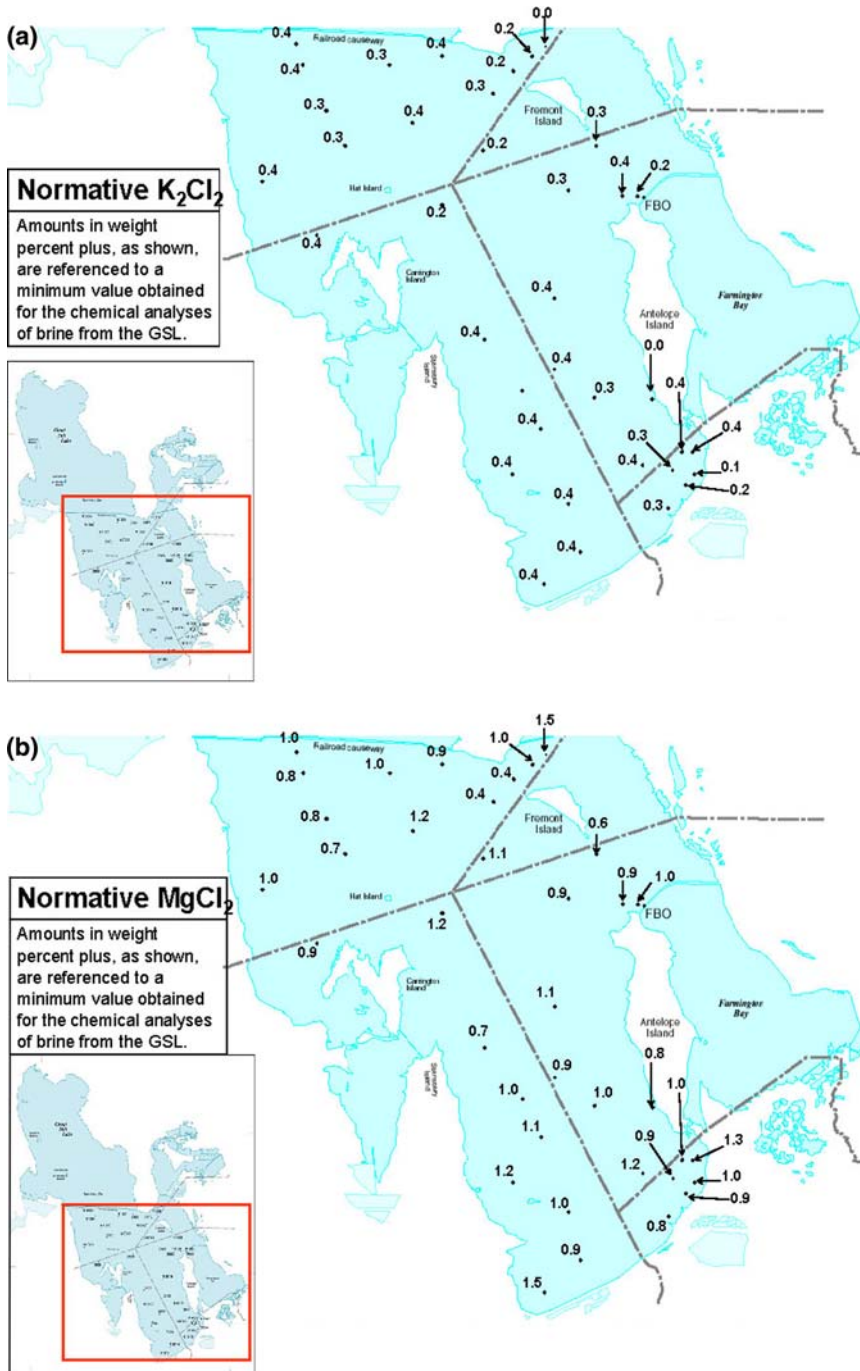


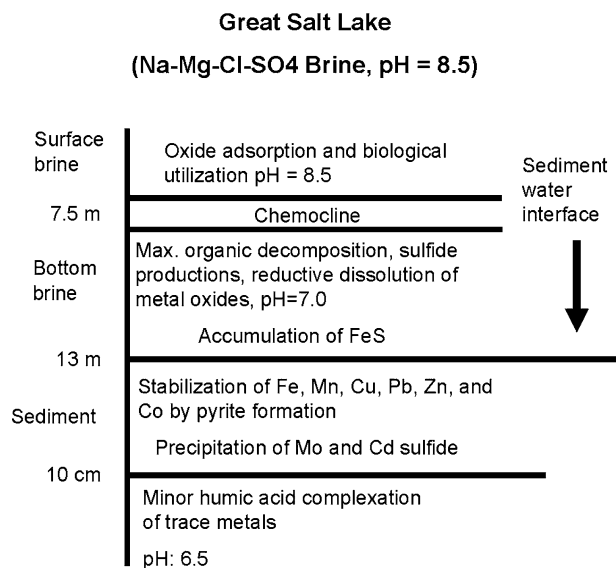
**Fig. 11** Amounts in weight percent of normative KCl (a) and  $MgCl_2$  (b) in excess of minimum value obtained for chemical analyses at lake water sampling sites in 2002

of the deviation of each site concentration from the lowest values at the time, which are used as a lake-wide reference. Comparison of these values suggests areas of dilute inflow, high evaporation, selective sorption, or unusual biotic activity. Note in the comparison of the GSL results that although both the residual major cations are relatively conservative in solution, the KCl concentration is nearly constant, whereas the  $MgCl_2$  values vary as one might expect for particular processes, e.g., low in areas of inflow dilution or sediment uptake, higher in regions of more intense evaporation.

Oxidation-reduction reactions are particularly important in controlling the distribution of minor metals in closed lake systems. The chemical stratification that is so common in large saline lakes, such as GSL, is influential in maintaining redox boundaries, across which reductive dissolution of metal oxides and anaerobic degradation of organic matter takes place. A representative redox depth profile for GSL is given in Fig. 12.

A significant example of the importance of redox processes to minor elements at GSL is the case of mercury. The high concentrations of Cl and Br in GSL may enhance the atmospheric deposition of Hg to the lake surface. Previous studies (Mason and Gill 2005) have shown that the presence of halogens such as Br and Cl in the marine boundary layer (MBL) can act as oxidizing agents that will transform the relatively inert  $Hg_0$  in the atmosphere to reactive gaseous Hg (RGHg). Once formed, RGHg has high deposition velocities and has been observed to be rapidly removed from the atmosphere in polar locations relative to  $Hg_0$  (Schroeder et al. 1998). The abundance of Br and Cl in the MBL above GSL may favor the formation of RGHg and enhance Hg deposition rates. Once inorganic forms of Hg enter GSL, the physical and chemical conditions may be ideal for Hg methylation. Previous work has shown that marine sediment rich in organic matter and dissolved sulfide have rapid  $CH_3Hg$  production rates in conjunction with rapid rates of  $SO_4$  reduction (King et al. 2000). Low dissolved  $O_2$  saturation in hypersaline systems such as GSL can support high rates of  $SO_4$  reduction. The  $SO_4$  reduction rates measured in GSL were higher than  $6000\text{ nmol/cm}^3/\text{day}$ , one of the highest rates reported in a natural environment (Ingvorsen and Brandt 2002). In laboratory experiments, King et al. (2000) determined that  $SO_4$  reducing bacteria capable of acetate utilization in their metabolic

**Fig. 12** Representative oxidation-reduction profile with depth at Great Salt Lake and its effects on the distribution of minor metals. From Domagalski et al. (1990)



pathways are the most efficient at methylating Hg. Acetate-utilizing bacteria (*Desulfobacter halotolerans* and *Desulfocella halophila*) capable of high methyl-Hg production have been isolated from sediment in the south arm of GSL (Ingvorsen and Brandt 2002).

Whole water samples were collected from GSL in 2003, 2005, and 2007 and analyzed for total Hg and CH<sub>3</sub>Hg. The highest concentrations of total Hg were found in water samples collected from the DBL, ranging from 7 to >100 ng/l (Naftz et al. 2008), with a median concentration of 42 ng/l. A significant proportion (31–60%) of the total Hg in water samples from the DBL was composed of CH<sub>3</sub>Hg. Concentrations of CH<sub>3</sub>Hg in the DBL ranged from 0.84 to >30 ng/l. The concentration of CH<sub>3</sub>Hg measured in GSL is among the highest measured in surface water by the USGS Mercury Research Laboratory. For comparison, CH<sub>3</sub>Hg in wholewater samples collected from Maryland reservoirs ranged from 0.007 to 0.493 ng/l (Mason and Sveinsdottir 2003).

Besides mixing and associated smaller scale processes (degassing, temperature change), evaporative concentration is the dominant mechanism effecting mineral formation and the solute evolution accompanying sequential mineral saturation and precipitation. The sequence is readily illustrated with a flow chart such as modified from Eugster and Hardie (1978) (Fig. 4) and based on relative solubility. Thus the first minerals to precipitate from GSL waters increasing in salinity are the alkaline-earth carbonates. The equilibrium precipitation of calcite helps illustrate a major control on the solute evolution of saline lake waters: the “chemical divide” (first defined by Hardie and Eugster 1970).

As discussed in the section on “concepts,” for the precipitation of pure mineral, cation and anion both contribute to the precipitate and are lost from the solution in equal proportion. At the same time, the solubility product of cation and anion must be constant, so as the mineral precipitates, unequal amounts remain in solution and the constituent of greater proportion will become dominant in solution on further concentration, i.e., increasing Ca will decrease the level of CO<sub>3</sub> or vice versa. Thus, early precipitation of calcite determines whether the remaining solution will become carbonate rich or poor.

As noted earlier, an effective technique for applying the “chemical divide” concept is the prediction of solute evolution through use of the “Spencer Triangle” (Fig. 5). To summarize the explanation given in the “concepts” section, in a triangular diagram of the system Ca-SO<sub>4</sub>(CO<sub>3</sub> + HCO<sub>3</sub>) a line connecting a point representing a particular solute distribution and a particular precipitate composition will define the direction of the chemical evolution of the water. The join between CaCO<sub>3</sub> and the SO<sub>4</sub> apex represents the calcite divide, and the join from CaCO<sub>3</sub> to CaSO<sub>4</sub> represents the gypsum divide. Solutions will move away from these divides as the respective minerals precipitate. NaCl is considered ubiquitous. Each triangular field is named according to the principle solutes left in the final fluid.

In application of these concepts to the chemical evolution at GSL (or any other saline lake) one must recognize solute loss by precipitation of salt. As a result, a flowchart pathway may be terminated or modified (Fig. 4). In the case of GSL, the solute evolution is complicated by at least three compositionally distinct inflow sources, which have contributed different proportions over time. The relationships of the major inflow compositions are quantitatively diagrammed in Fig. 13, whereas estimates of the total input over 35,000 years are given in Table 3. The model reveals differences in mineral precipitation sequence depending on low versus high inflow discharge. This is similar to the contrast between the present halite-dominant precipitation regime and the importance of mirabilite precipitation at low levels following highstands of pre-historic periods.

Other factors that have influenced salt precipitation sequence are temperature, Ca/Mg ratio, and sulfate reduction. Spencer et al. (1985b) have suggested that mirabilite beds of

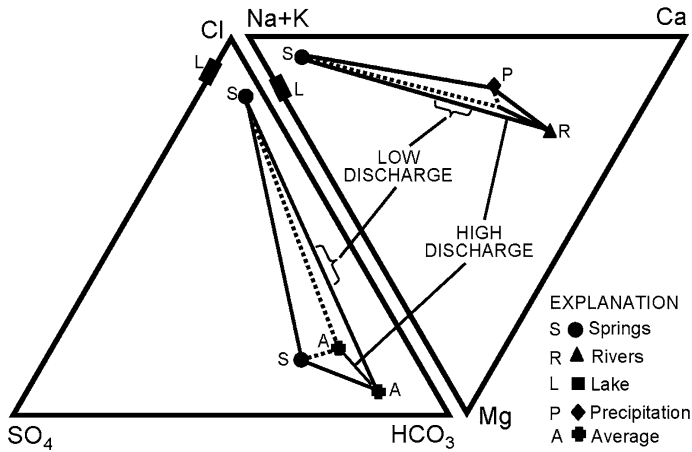


**Fig. 13** Inflow compositions (mole fraction). The springs (S) are NaCl rich, while the river waters (R) and precipitation (P) are Ca–HCO<sub>3</sub>–SO<sub>4</sub> rich. (A) is estimated composition of inflow over the past 35000 years. The present lake waters (L) require the removal of Ca, Mg, HCO<sub>3</sub>, and SO<sub>4</sub> from the inflow (from Spencer et al. 1985a)

the north basin formed during winter “chill out” (which has been observed temporarily in recent times) and were possibly protected from dissolution by stratification resulting from mineral precipitation. The marked decrease in the solubility of mirabilite below 25°C in temperature also can account for its formation rather than Mg sulfates (see Fig. 14) as the next step in the flowchart sequence, despite the rapid rise in Mg concentration accompanying evaporative concentration (partially damped by lesser losses of solute Mg to carbonate and Mg silicate). Because of increased Mg, the concentration of Ca and HCO<sub>3</sub> are controlled by aragonite rather than calcite. Continued high input of Cl and Na from

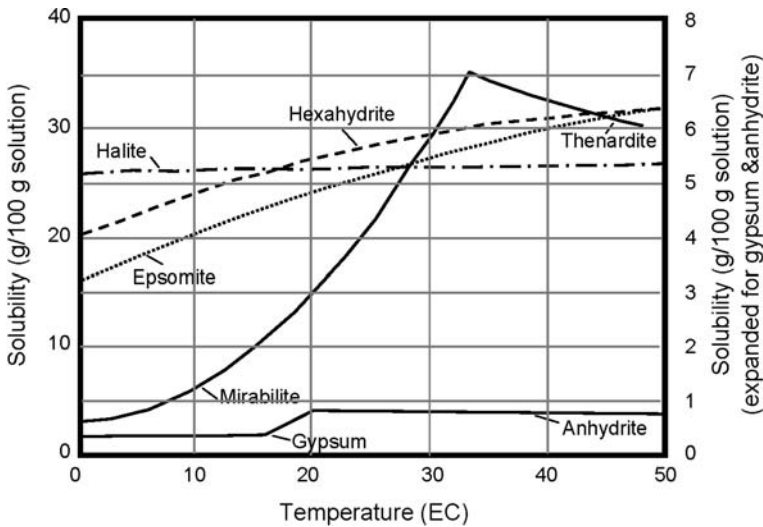


**Fig. 14** Temperature effects on the solubility of several important evaporate mineral phases, from Last (1999). Note that above about 28°C, mirabilite is more soluble than epsomite

hydrothermal sources and re-cycling from peripheral mud flats results in increased concentration in the lake, despite downward diffusion gradients (Fig. 8). In contrast, the diffusive fluxes of  $\text{SO}_4$ , K, and Mg into the sediment are supplemented or enhanced by diagenetic reactions in the sediment or stratification based on density contrast. Thus input of  $\text{SO}_4$ , K, and Mg is basically insufficient to keep up with removal. Sulfate reduction and some gypsum formation takes place variously in the sediment, whereas K fixation and Mg-silicate formation occurs throughout the clay fraction (Jones and Spencer 1999).

In historic time the lake seems to have passed through the  $\text{CaCO}_3$  divide repeatedly. As a result, carbonate precipitation processes have left the residual brines strongly enriched in Mg, depleted in Ca, and impoverished in bicarbonate. Mirabilite still occurs intermittently through brine chilling. According to Spencer et al. (1985b) the sequence expected from modern brines at  $25^\circ\text{C}$  is aragonite, small amounts of gypsum, a little glauberite, and then a large mass of halite. The variations in mineral precipitate sequences, the fossil mirabilite found in the sediment, and the halite dominance in salts precipitated at present are a testimony to the changing influence of input sources and sinks through time (Spencer et al. 1985b).

## 8 Summary and Conclusions

The GSL is the largest saline lake of North America, and its brines are some of the most concentrated anywhere in the world. The lake occupies a closed basin system whose chemistry reflects solute inputs from the weathering of rocks ranging in age from Precambrian and Paleozoic in the high mountains on the east to Tertiary and Quaternary sediments in the desert basins to the west. Lithologies cover a complete range including crystalline rocks (both intrusive and metamorphic), clastic sediments of all types, large sections of carbonates, and small sections of both marine and lacustrine evaporites. GSL is the remnant of a much larger lacustrine body, Lake Bonneville, and its geochemical evolution can be considered to have begun with the drop in the level of Bonneville at the end of the Pleistocene. Evidence of the effect of evaporative concentration (and  $\text{CaCO}_3$  precipitation) on high stand waters can be readily seen in the tufa deposits on older shorelines.

The water balance of GSL depends primarily on the inflow from three major rivers draining the ranges to the east and precipitation directly on the lake. The greatest solute inputs are from calcium bicarbonate river waters mixed with sodium chloride type springs and groundwaters. Prior to 1930, the lake concentration inversely tracked lake volume, which reflected climatic variation in the drainage. However, since that time, salt precipitation, primarily halite and mirabilite, and re-solution have periodically modified lake brine chemistry through density stratification and formation of brine pockets and compositional differentiation. In addition, construction of a railway causeway has restricted circulation, nearly isolating the northern from the southern part of the lake, which receives 90% of the inflow, leading to halite precipitation in the north. Widespread halite precipitation occurred prior to railroad-causeway construction, especially in the south, as a result of severe droughts. The presence of a mid-lake subaqueous ridge, probably had the same effect. These conditions have emphasized brine differentiation, mixing, and fractional precipitation of salts as major factors in solute evolution, especially in relatively shallow systems.

The work at GSL has also highlighted the role of pore fluids as sources and sinks of solutes in the lake, depending on the concentration gradient. Also, diagenetic reactions in the sediments cause gypsum to precipitate or dissolve irregularly because calcium levels

are so low after extensive carbonate deposition. Alkalinity and low calcium concentrations are usually near constancy at aragonite rather than calcite saturation, because of increasing Mg/Ca ratio. In addition to carbonate, significant amounts of dissolved Mg and K are lost to clays through diagenetic pore-fluid reactions. Accounting for pore-fluid diffusion has permitted a reasonable balance to be made between solute input over time and the quantities now found in solution and sediments. Excess amounts of calcium, carbonate, and silica can be attributed to detrital input.

Comparison of analyzed and computer determinations of a halite-saturated pond sequence from GSL indicated similar points of crystallization for minor salt phases. Compositional plots of major ions versus bromide suggested bitter salt (kainite) uptake of Br began at 700 ppm (as compared to 70 ppm for halite), and computer calculations produced solubility values for phases subsidiary to halite in the GLS evaporative pond sequence.

## References

- Arnou T, Stephens D (1990) Hydrologic characteristics of the Great Salt Lake, Utah: 1847–1986. US Geol Surv Water Supply Pap 2332:32
- Balch DP, Cohen AS, Schnurrenberger DW et al (2005) Ecosystem and paleohydrological response to quaternary climate change in the Bonneville basin, Utah. *Palaeogeogr Palaeoclimatol Palaeoecol* 221:99–122. doi:[10.1016/j.palaeo.2005.01.013](https://doi.org/10.1016/j.palaeo.2005.01.013)
- Baskin RL, Allen DV (2005) Bathymetric map of the south part of Great Salt Lake. Utah. US Geol Surv Sci Invest Map, 2894
- Bodine MW Jr, Jones BF (1986) The salt norm: a quantitative chemical-mineralogical characterization of natural waters. U.S. Geol Surv Water Res Inves Rep 86-4086
- Cole DR (1982) Tracing fluid sources in the East Shore Area, Utah. *Ground Water* 20:586–592. doi:[10.1111/j.1745-6584.1982.tb01374.x](https://doi.org/10.1111/j.1745-6584.1982.tb01374.x)
- Currey DR (1990) Quaternary paleolakes in the evolution of semidesert basins, with special emphasis on Lake Bonneville and the Great Basin. *USA Palaeogeogr Palaeoclim Palaeoecol* 76:189–214. doi:[10.1016/0031-0182\(90\)90113-L](https://doi.org/10.1016/0031-0182(90)90113-L)
- Domagalski JL, Eugster HP, Jones BF (1990) Trace metal geochemistry of Walker, Mono, and Great Salt Lakes. In: Spencer RJ, Chou IM (eds) *Fluid–mineral interaction: a tribute to H.P. Eugster*. The Geochem Society, Special Publ. 2, pp 315–353
- Eugster HP, Hardie LA (1978) Saline lakes. In: Lerman A (ed) *Lakes: chemistry, geology, physics*, chap 8. Springer, New York, pp 237–293
- Eugster HP, Jones BF (1979) Behavior of major solutes during closed-basin brine evolution. *Am J Sci* 279:609–631
- Feth JH (1960) Re-evaluation of the salt chronology of several Great Basin lakes: a discussion. *Geol Soc Am Bull* 30:637–640
- Fuchtbauer H, Hardie LA (1976) Experimentally determined homogenous distribution coefficients for precipitated magnesian calcites; application to marine carbonate cements. *Geol Soc Am (Abst Prog)*, 876–877
- Gilbert GK (1890) *Lake Bonneville*. Monograph 1, US Geological Survey, Washington, 340 p
- Godsey HS, Currey DR, Chan MA (2005) New evidence for an extended occupation of the Provo shoreline and implications for regional climate change, Pleistocene Lake Bonneville, Utah, USA. *Quat Res* 63:212–223. doi:[10.1016/j.yqres.2005.01.002](https://doi.org/10.1016/j.yqres.2005.01.002)
- Gwynn JW (2002) Great Salt Lake, Utah: chemical and physical variations of the brine and effects of the SPRR causeway, 1966–1996. In: Gwynn JW (ed) *Great Salt Lake, an overview of change*. Utah Dept Nat Res Spec Pub., 584 pp
- Hahl DC, Handy AH (1969) Great Salt Lake, Utah: a chemical and physical variation of the brine 1963–1966. *Utah Geological Mineralogical Survey Water-Resources Bulletin* 12, 33 p
- Hahl DC, Mitchell CG (1963) Dissolved-mineral inflow to Great Salt Lake and chemical characteristics of the Salt Lake brine: part 1, selected hydrologic data. *Utah Geological Mineralogical Survey Water-Resources Bulletin* 3, 40 p
- Hardie LA, Eugster HP (1970) The evolution of closed basin brines. *Min Soc Am Spec Pub* 3:273–290

- Ingvorsen K, Brandt KK (2002) Anaerobic microbiology and sulfur cycling in hypersaline sediments with special reference to Great Salt Lake. In: Gwynn JW (ed) Great Salt Lake: an overview of change. Utah Department of Natural Resources Special Publication. Salt Lake City, Utah, pp 387–398
- Jones BF (1966) Geochemical evolution of closed basin water in the western Great Basin. In: Rau JL (ed) 2nd Symposium on Salt. North. Ohio Geological Society, vol 1, pp 181–200
- Jones BF, Bodine MW (1987) Normative salt characterization of natural waters. In: Fritz P, Frape SK (eds) Saline waters and gases in crystalline rocks. Geological Association of Canada Special Paper 33, pp 5–18
- Jones BF, Deocampo DM (2003) Geochemistry of saline lakes. In: Drever JI, Holland HD, Turekian KK (eds) Freshwater geochemistry, weathering and soils. Treatise on Geochemistry, vol 5.13, pp 393–424
- Jones BF, Spencer RJ (1999) Clay mineral diagenesis at Great Salt Lake, Utah, USA. 5th International symposium on the geochemistry of the earth's surface. Reykjavik, Iceland. Balkema, Rotterdam, pp 293–297
- Jones BF, Carmody R, Frape SK (1997) Variations in principal solutes and stable isotopes of Cl and S on evaporation of brines from the Great Salt Lake, Utah. *Geol Soc Am Abs Prog* 29:261
- King JK, Kostka JE, Frischer ME et al (2000) Sulfate reducing bacteria methylate mercury at variable rates in pure culture and marine sediments. *Appl Environ Microbiol* 66:2430–2437. doi:[10.1128/AEM.66.6.2430-2437.2000](https://doi.org/10.1128/AEM.66.6.2430-2437.2000)
- Kohler JF, White WW III (2004) Characteristics of the near-surface brine resources in the Newfoundland Basin, Tooele and Box Elder Counties, Utah. In: Castor SB, Papke KG, Meeuwig RO (eds) Betting on industrial minerals, proceedings of the 39th forum on the geology of industrial minerals, vol 33, pp 181–187. Nev Bu Mines & Geology, Sparks, Nevada
- Kowalewska A, Cohen AS (1998) Reconstruction of paleoenvironments of the Great Salt Lake basin during the late Cenozoic. *J Paleolimnol* 20:381–407. doi:[10.1023/A:1008053505320](https://doi.org/10.1023/A:1008053505320)
- Last WM (1999) Geolimnology of the Great Plains of western Canada. In: Lemmen DS, Vance RE (eds) Holocene climate and environmental change in the Palliser triangle: a geoscientific context for evaluating the impacts of climate change on the southern Canadian prairies. *Geol Surv Can Bull*, vol 534, pp 23–55
- Mason RP, Gill GA (2005) Mercury in the marine environment. In: Parsons MB, Percival JB (eds) Mercury: sources, measurements, cycles, and effects. Mineralogical Association of Canada, vol 34, pp 79–216
- Mason RP, Sveinsdottir AY (2003) Mercury and methylmercury concentrations in water and largemouth bass in Maryland reservoirs. [http://www.dnr.state.md.us/streams/pubs/ad-03-1\\_Hg\\_bass.pdf](http://www.dnr.state.md.us/streams/pubs/ad-03-1_Hg_bass.pdf). Accessed 22 November 2004
- Miller DM (1991) Mesozoic and Cenozoic tectonic evolution of the northeastern Great Basin. In: Buffa RH, Conyer AR (eds) Geology and ore deposits of the Great Basin. *Geol Soc Nev, Reno Nevada*, pp 202–228
- Møller N, Weare JH, Duan Z, Greenberg JP (1997) Chemical models for optimizing geothermal energy production: Unpublished Internet document, U.S. Department of Energy Technical Site, Research Summaries-Reservoir Technology
- Naftz DL, Angerth C, Kenney T, Waddell B, Silva S, Darnall N, Perschon C, Whitehead J (2008) Anthropogenic influences on the input and biogeochemical cycling of nutrients and mercury in Great Salt Lake, Utah, USA. *Appl Geochem* 23:1731–1744. doi:[10.1016/j.apgeochem.2008.03.002](https://doi.org/10.1016/j.apgeochem.2008.03.002)
- O'Connor JE (1993) Hydrology, hydraulics, and geomorphology of the Bonneville flood *Geol Soc Am Spec Paper* 274, 83 pp
- Oviatt CG (1997) Lake Bonneville fluctuations and global climate change. *Geology* 25:155–158 doi:[10.1130/0091-7613\(1997\)025<0155:LBFAGC>2.3.CO;2](https://doi.org/10.1130/0091-7613(1997)025<0155:LBFAGC>2.3.CO;2)
- Oviatt CG, Currey DR, Sack D (1992) Radiocarbon chronology of Lake Bonneville, eastern Great Basin, USA. *Palaeogeogr Palaeoclimatol Palaeoecol* 99:225–241. doi:[10.1016/0031-0182\(92\)90017-Y](https://doi.org/10.1016/0031-0182(92)90017-Y)
- Oviatt CG, Habiger GD, Hay JE (1994) Variation in the composition of Lake Bonneville marl: a potential key to lake-level fluctuations and paleoclimate. *J Paleolimnol* 11:19–30. doi:[10.1007/BF00683268](https://doi.org/10.1007/BF00683268)
- Oviatt CG, Miller DM, McGeehin JP et al (2005) The younger Dryas phase of Great Salt Lake, Utah, USA. *Palaeogeogr Palaeoclimatol Palaeoecol* 219:263–284. doi:[10.1016/j.palaeo.2004.12.029](https://doi.org/10.1016/j.palaeo.2004.12.029)
- Pedone VA (2004) Paleohydrology of Lake Bonneville determined by mineralogy and C, O, and Sr isotope compositions of authigenic carbonates. *Geol Soc Am Abs Prog* 36:472
- Schroeder WH, Anlauf KG, Barrie LA, Lu JY, Steffen A, Schneeberger DR, Berg T (1998) Arctic springtime depletion of mercury. *Nature* 394:331–333. doi:[10.1038/28530](https://doi.org/10.1038/28530)
- Scott WE, McCoy WD, Shroba RR et al (1983) Reinterpretation of the exposed record of the last two cycles of Lake Bonneville, western United States. *Quat Res* 20:261–285. doi:[10.1016/0033-5894\(83\)90013-3](https://doi.org/10.1016/0033-5894(83)90013-3)
- Spencer RJ, Hardie LA (1990) Control of seawater composition by mixing of river waters and mid-ocean ridge hydrothermal brines. In: Spencer RJ, Chou IM (eds) Fluid–mineral interaction: a tribute to H. P. Eugster. *The Geochem Soc Spec Pub* vol 2, pp 409–419

- Spencer RJ, Baedecker MJ, Eugster HP et al (1984) Great Salt Lake and precursors, Utah: the last 30,000 years. *Con Min Pet* 86:321–334. doi:[10.1007/BF01187137](https://doi.org/10.1007/BF01187137)
- Spencer RJ, Eugster HP, Jones BF et al (1985a) Geochemistry of Great Salt Lake, Utah I: hydrochemistry since 1850. *Geochem Cosmochem Acta* 49:727–737. doi:[10.1016/0016-7037\(85\)90167-X](https://doi.org/10.1016/0016-7037(85)90167-X)
- Spencer RJ, Eugster HP, Jones BF (1985b) Geochemistry of Great Salt Lake, Utah II: pleistocene-holocene transition. *Geochem Cosmochem Acta* 49:739–747. doi:[10.1016/0016-7037\(85\)90168-1](https://doi.org/10.1016/0016-7037(85)90168-1)
- Thompson RS, Toolin LJ, Forester RM et al (1990) Accelerator-mass spectrometer (AMS) radiocarbon dating of Pleistocene lake sediments in the Great Basin. *Palaeogeogr Palaeoclimatol Palaeoecol* 78:301–313
- Zdanowicz CM, Zielinski GA, Germani MS (1999) Mount Mazama eruption: calendrical age verified and atmospheric impact assessed. *Geology* 27:621–624 doi:[10.1130/0091-7613\(1999\)027<0621:MMECAV>2.3.CO;2](https://doi.org/10.1130/0091-7613(1999)027<0621:MMECAV>2.3.CO;2)